Title
SIMULTANEOUS MEASUREMENTS OF ATMOSPHERIC EMISSIONS AT 10, 33, AND 90 GHz

Author
Costales, J.B.

Publication Date
1984-11-01

Lawrence Berkeley Laboratory
UNIVERSITY OF CALIFORNIA

Physics Division

Submitted to Radio Science

SIMULTANEOUS MEASUREMENTS OF ATMOSPHERIC
EMISSIONS AT 10, 33, and 90 GHz

J.B. Costales, G.F. Smoot, C. Witebsky,
G. De Amici and S.D. Friedman

November 1984

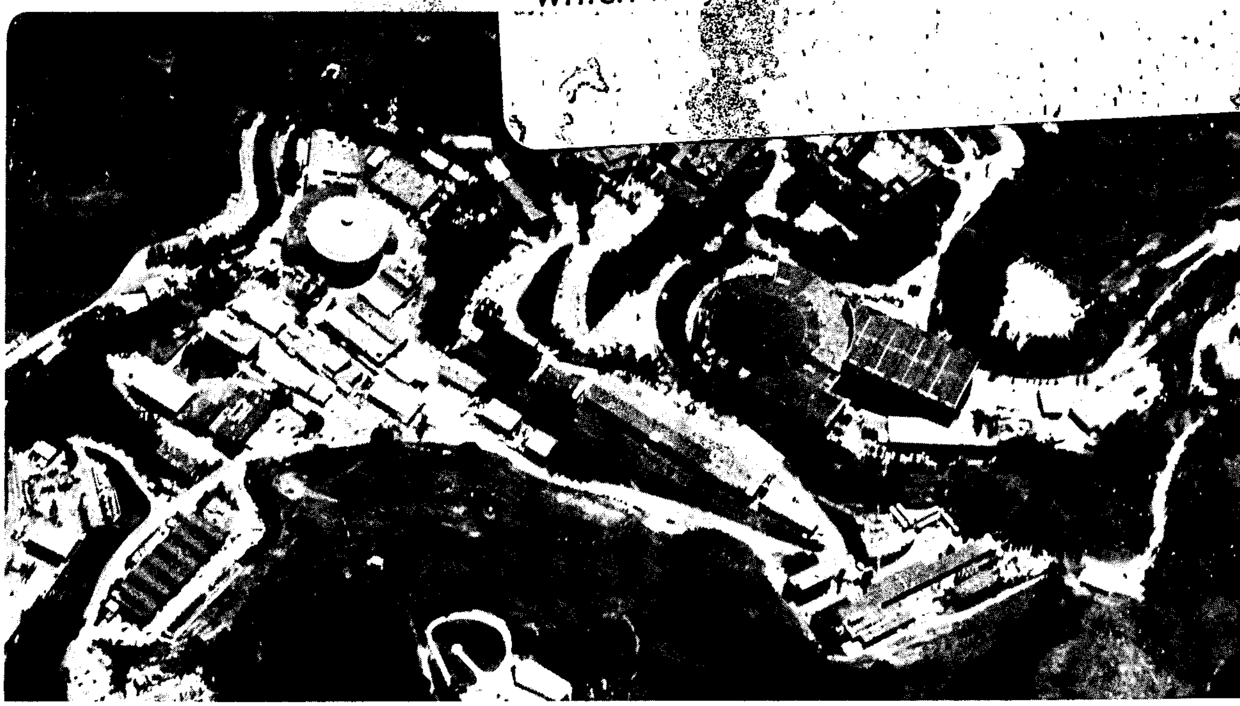

Prepared for the U.S. Department of Energy under Contract DE-AC03-76SF00098

SIMULTANEOUS MEASUREMENTS OF ATMOSPHERIC EMISSIONS AT 10, 33 AND 90 GHZ

James B. Costales, George F. Smoot, Chris Witebsky, Giovanni De Amici and Scott D. Friedman
Lawrence Berkeley Laboratories, University of California,
Berkeley, CA 94720

ABSTRACT

As part of a larger experiment to measure the cosmic microwave background radiation spectrum, frequent simultaneous measurements of the microwave thermal emissions from the earth's atmosphere were made at 10 GHz, 33 GHz and 90 GHz. We performed these measurements at two separate locations, Berkeley, California and the White Mountain Research Station (located near Bishop, California) which differed greatly in altitude and climatic conditions. Typical values of the atmospheric antenna temperature measured in Berkeley (250 m elevation) during good weather are 2.54±0.29 K, 12.4±0.3 K and 34.3±0.5 K for 10, 33 and 90 GHz respectively. Corresponding values measured at White Mountain (3800 m) are 1.11±0.04 K, 4.48±0.18 K and 11.0±0.1 K. Because the measurements are simultaneous in nature, correlations between the measurements taken at the various frequencies provide constraints on models of the microwave emission of the earth's atmosphere, especially models describing atmospheric emission as a function of precipitable water content.

1. INTRODUCTION

As a source of noise and attenuation, the atmosphere plays a significant role in fields such as radio frequency communications, remote microwave sensing and radioastronomy [Crane, 1981]. For example, precise measurements of the cosmic microwave background spectrum are severely restricted not only by galactic emissions but also by atmospheric emissions mainly due to rotational transitions of molecular oxygen and water. To reduce the galactic contributions to negligible levels, one generally measures the spectrum at frequencies greater than about 2 GHz and at positions on the sky away from the galactic plane. To reduce atmospheric emission fluctuations and magnitudes, one generally uses a high altitude site, though the intensities remain significant, even at frequencies corresponding to atmospheric windows. A good understanding of the atmospheric absorption and emission is therefore essential to making atmospheric corrections for the spectrum measurements.

Much progress has been made in understanding and calculating the functional dependence of the atmosphere's opacity or emission on frequency, pressure and temperature. Scattering is generally negligible at microwave frequencies, especially during clear weather, so that we may use attenuation and emission interchangeably in this paper. One calculates the atmospheric emission (brightness or antenna temperature) $T_{A,atm,\nu}$ at a frequency ν by computing the radiative transfer integral, i.e.

$$T_{A,atm,\nu} = \int_0^s J_\nu(s') \exp\left[-\int_{s'}^{s} \kappa_\nu(s'')ds''\right]\kappa_\nu(s')ds', \tag{1}$$

where s corresponds to the point of observation, κ_ν is the specific attenuation coefficient at frequency ν, and J_ν is the source function [Waters, 1976]. At microwave frequencies the atmosphere is approximately non-scattering and in thermal equilibrium, so one may use the blackbody formula (expressed in Kelvin) for the source function. The power P received by an antenna is related to the antenna temperature T_A of the incoming radiation by

$$P = kT_A B, \tag{2}$$

where k is Boltzmann's constant and B is the bandwidth of the receiver.

Figures 1 and 2 display evaluations of equation (1) (see Section 5 for details of the model used) and corresponding measurements made at altitudes of 250 m and 3800 m. Such calculations being quite tedious, it is useful to simplify equation (1) using several good approximations. Since the physical atmospheric temperature and the blackbody function are approximately equal for frequencies less than 100 GHz ($h\nu << kT$) and since the relative temperature dependencies of the integrand are small, one may replace J_ν by T_{phys} (about 250 K), the average physical temperature of the atmosphere. Performing the integral, one obtains

$$T_{A,atm,\nu} = T_{phys}[1 - \exp(-\kappa_{\nu,H_2O} - \kappa_{\nu,O_2})], \tag{3}$$

where the specific attenuation coefficient has been separated into its oxygen and water components. In the atmospheric windows and at frequencies below 18 GHz, the atmosphere is optically thin (see Figures 1 and 2) so that we may expand the exponential keeping only the linear terms. Because the pressure and temperature variations of oxygen are generally small at a given altitude, the oxygen term may be expressed as a constant. The resulting calculated atmospheric emission may be written as

$$T_{A,atm,\nu} = a_\nu + b_\nu W, \tag{4}$$

where a_ν is the oxygen term, b_ν the water coefficient, and W [mm] the precipitable water content. Although a_ν and b_ν depend on the ambient conditions of the atmosphere, these dependencies are relatively weak for the fluctuations in dry air pressure and ambient temperature observed and hence the terms may be generally considered as functions of altitude only.

Equation (4) indicates that atmospheric emissions at frequencies where the atmosphere is relatively transparent should be linearly correlated. To verify this and to determine the correlation parameters, we performed frequent simultaneous measurements of the atmospheric thermal emissions at 10, 33 and 90 GHz at Berkeley, California and White Mountain, California. Partridge *et al.* [1984] reported some of our previous results at White Mountain in addition to their measurements at 9.4 GHz. In addition to providing corrections essential to the CBR spectrum experiment, these measurements, being simultaneous, not only help to check the validity of atmospheric models used to make the correction, but also constrain models of the microwave emission by the earth's atmosphere.

2. CONCEPTS AND DESIGN OF THE EXPERIMENT

The intensity of atmospheric emission is measured at a fixed frequency by a radiometer, an instrument whose output signal is proportional to the power received by the antenna. We measure the calibration constant by simultaneously looking with each radiometer at two targets whose temperatures widely differ and are known to sufficient accuracy. As cold reference loads, we used either a liquid helium- or liquid nitrogen-cooled target or the zenith sky. The cold load cryostat has been described previously [Smoot *et al.*, 1983] and has not been significantly modified. In addition, each radiometer has an ambient-temperature blackbody load used as a warm reference load.

One determines the thermal contributions from the atmosphere by measuring the antenna temperature of the incoming radiation at various known zenith angles. Several sources of emission comprise the total power received by the antenna. To a good approximation, the power $T_{A,\nu}(\theta)$ received by an antenna at frequency ν when directed at an angle θ from the zenith is given by

$$T_{A,\nu}(\theta) = T_{A,atm,\nu}(\theta) + T_{A,CBR,\nu} + T_{ground,\nu}(\theta) + T_{galaxy,\nu}(\theta), \tag{5}$$

where $T_{A,atm,\nu}(\theta)$ is the antenna temperature of the atmosphere, $T_{A,CBR,\nu}$ is the antenna temperature of the cosmic background radiation (CBR), $T_{ground,\nu}(\theta)$ is the antenna temperature of the terrestrial thermal radiation intercepted by the antenna sidelobes, and $T_{galaxy,\nu}(\theta)$ is the antenna temperature of the radiation from the galaxy. At frequencies where the atmosphere is optically thin, the atmospheric emission observed at a zenith angle θ, is approximately proportional to the path length of air looked through, so $T_{A,atm,\nu}(\theta)$ is approximately the product of the secant of the zenith angle $\sec(\theta)$ and the vertical atmospheric antenna temperature $T_{A,atm,\nu}(0)$.

By making differential measurements with the zenith sky as a reference source, one may reduce the uncertainty in determining the atmospheric emission, since for isotropic sources, such as the CBR, one must then only account for the difference in attenuation (< 40 mK) along the reference and source paths. Although not isotropic, contributions from the galaxy are generally very small (< 8 mK for frequencies greater than 10 GHz), especially if one avoids directing the antennas at the galactic plane, the sun and the moon. The contributions from the antenna sidelobes, greatly reduced through the use of corrugated-horn antennas and ground screens, can nevertheless be measured and are generally also relatively small (< 20 mK). Because the antennas have a finite beam width, the calculation of $T_{A,atm,\nu}(0)$ must involve convolving the measured antenna beam pattern with the atmosphere, at the same time accounting for the curvature of the atmosphere and atmospheric self-absorption.

For some of our measurements, it is necessary to use mirrors to redirect the incoming radiation to the antennas of the radiometers. In general one must account for the fact that the reflectors' emissivity is a function of angle. To greatly reduce the angular dependency of the detected reflector emission we used a receiver which only accepts circularly polarized radiation at 10 GHz and adjusted the planes of polarization at 33 GHz to minimize the effect. The typical residual correction was 23 and 60 mK, respectively. The 90 GHz radiometer did not use mirrors in these measurements; the antenna pointed directly at the sky.

All three radiometers have superheterodyne receivers operated with Dicke switching, conically shaped low-sidelobe corrugated-horn antennas, thermal control systems, ground screens and mirrors. All three radiometers share the same power supplies, digital recording system and cold-load dewar. The sensitivities of the radiometers range from 50–90 mK/Hz$^{1/2}$. Previous papers [Friedman *et al.*, 1984; De Amici *et al.*, 1984; Smoot *et al.*, 1985] describe the radiometers in greater detail.

In order to check the performance of the radiometers several tests were performed, some of which were periodically repeated. These tests include magnetic sensitivity tests, motion/orientation sensitivity tests, integration tests, gain stability and linearity tests, side lobe tests and RF interference tests. All of the tests yielded acceptable results, some of which were used to calculate experimental corrections and uncertainties.

3. OBSERVATIONS AND DATA REDUCTION

During the summer months of 1984, we measured the atmospheric emissions several times a week at the Lawrence Berkeley Laboratories located about 250 m above sea level. Our measurements were made under a variety of weather conditions. Typical values for the ambient temperature and barometric pressure were 15–24 °C and 746 mm Hg, respectively.

We carried out our CBR spectrum measurements during August of 1984 at the University of California's high-altitude White Mountain Research Station located near Bishop, California on a plateau at an elevation of 3800 m. Because of the high altitude and semi-arid climate of the site, the atmospheric emission is greatly reduced. The typical column density of precipitable water (3 mm) is roughly one-third the minimum column density at Berkeley. Typical values for the ambient temperature and barometric pressure were 2–10 °C and 490 mm Hg.

During a single sequence each radiometer measures the atmospheric intensity at 4–6 angles in the north-south vertical plane (or, in the case of the 10 GHz radiometer, the east-west vertical plane). The essential features of a sequence, in addition to measuring the intensity as a function of angle, are measurements of the gain and instrumental offset.

The Berkeley data in general were read directly from voltmeters and recorded by hand.

The 33 GHz data taken at Berkeley during the summer were for the most part analyzed using a simple secant model which neglects the attenuation of the CBR, curvature of the atmosphere, and the finite beam width of the antenna pattern. In general these corrections are small (< 20 mK) and are of a lower order of magnitude than the fluctuations observed.

Similarly, the data taken at the White Mountain Research Station were first analyzed in the field in this manner. These rough calculations in real time allow us to identify any problems if they should arise. At White Mountain we used a Datel data logger which automatically recorded radiometer output and target temperatures onto magnetic tape. Data files constructed from these tapes were edited by hand to delete data recorded while the mirrors or targets were being positioned. Computer programs customized for each radiometer analyzed the data files, computing atmospheric emission and cosmic background intensity for each sequence.

In general, systematic errors determine the accuracy of the measurements. especially at White Mountain where the atmospheric fluctuations are minimal, The uncertainties in the gain, pointing angles and mirror emissivity are the largest sources of systematic error. The uncertainties in the antenna beam pattern, sidelobe contributions, average atmospheric temperature and atmospheric scale height are smaller sources of experimental uncertainty taken into account. We estimate the total systematic uncertainties in our atmospheric measurements to be 120 mK, 90 mK and 180 mK respectively, for the frequencies of 10, 33 and 90 GHz.

4. RESULTS

The atmospheric emission at frequencies ν_x and ν_y may be expressed as

$$T_{A,atm,\nu_x} = a_{\nu_x} + b_{\nu_x} W \tag{6a}$$

$$T_{A,atm,\nu_y} = a_{\nu_y} + b_{\nu_y} W, \tag{6b}$$

or, eliminating the precipitable water content W,

$$T_{A,atm,\nu_y} = \alpha_{\nu_y,\nu_x} T_{A,atm,\nu_x} + \beta_{\nu_y,\nu_x}. \tag{7}$$

The slopes and the intercepts are related to the coefficients by:

$$\alpha_{\nu_y,\nu_x} = b_{\nu_y}/b_{\nu_x} \tag{8a}$$

$$\beta_{\nu_y,\nu_x} = a_{\nu_y} - a_{\nu_x}\alpha_{\nu_y,\nu_x}. \tag{8b}$$

Thus the α's serve to constrain the relative water coefficients, whereas both the α's and the β's constrain the oxygen contributions at the respective frequencies.

Our results strongly confirm the linear correlation suggested by equations (4) and (7). Figures 3–5 show the results of our Berkeley measurements. Each point on the figures corresponds to the average measured atmospheric temperature during a sequence (4–6 points). Since the number of measurements made over a sequence is small, the standard deviation of the data may not in some cases give one a good idea of the statistical error. To overcome this, statistical errors were averaged over a set of consecutive measuring sequences. The resulting averages were then summed in quadrature with the system noise fluctuations.

The fluctuations due to the variability of the atmospheric conditions, i.e. relative humidity, are evident in these figures. Average clear-night values of the atmospheric antenna temperature are 2.54 ± 0.29 K, 12.4 ± 0.3 K, and 34.3 ± 0.5 K, in order of increasing frequency. Since there are obvious deviations resulting from higher order terms and possible attenuation and scatter by liquid water [Ulaby, 1981], the best-fit lines are drawn through the points representing clear weather. Attenuation due to liquid water theoretically should be observable at some level since the attenuation due to liquid water and the attenuation due to water vapor (dominated by the empirical term) have different dependencies on frequency [Ulaby, 1981]. Unfortunately, the low number of points taken during foggy or cloudy nights as well as the scatter and large errors in the ones that were taken prevent us from obtaining a quantitative result for the coefficients of the higher order terms (W^2) or the extra attenuation resulting from liquid water. The scatter of these points as well as their large uncertainties reflect the spatial and temporal variability of the atmospheric conditions on time scales smaller than the time it takes to perform a set of measurements (4–6 minutes).

The errors quoted in the figures represent quadrature sums of best-fit uncertainties and systematic errors. To calculate the systematic uncertainty of these measurements we have considered two general types of errors: those which would merely shift the line without affecting its slope; and those which would change the scale (stretch or shrink) thereby changing the slope and the intercept. The first type of error (offset errors) includes uncertainties in the physical temperature of the atmosphere (leading to an uncertainty < 16 mK at each frequency), atmospheric scale height (< 15 mK), pointing angles (< 45 mK), sidelobe contributions (< 20 mK) and mirror emissivity (< 60 mK). The second type (scale errors) include uncertainties in the gain ($< 2\%$) and beam pattern ($< 1\%$).

Figures 6–8 show our results for our White Mountain measurements. Generally, the average statistical fluctuations of a given sequence were larger than the noise of the system. Quite noticable in these figures, especially in Figure 8, are the regions corresponding to various weather conditions, i.e. clear weather (lower left), foggy weather (middle region), and cloudy weather (upper right hand corner). Typical values of the atmospheric antenna temperature during good weather ranged between about 1.02–1.47 K at 10 GHz, 3.95–7.05 K at 33 GHz, and 9.1–13.8 K at 90 GHz. These measurements are consistent with other measurements made at White Mountain about the same time of year. At frequencies of 9.4 GHz [Wilkinson, 1967] and 35 GHz [Stokes *et al.*, 1967], the measured vertical atmospheric antenna temperatures ranged from 1.32 to 1.49 K and 5.71 to 7.68 K, respectively. Ewing *et al.* [1967] reported their measurements of $T_{A,atm}(0)$ at 32.5 GHz to lie in the range 3.29–5.59 K. More recently Partridge *et al.* [1984] measured the atmospheric contribution at 9.4 GHz to range from 0.89 to 1.23 K. Although the measurements by Stokes *et al.* and Wilkinson seem to be a little high, as noted by Partridge *et al.* [1984], they still fall within the ranges we observed during clear weather.

Figures 6–8, especially Figure 8 where the effect should be most noticable, do not reveal any clear indications of additional attenuation due to higher-order terms or due to liquid water. However, the large scatter in the points and the lack of significant amounts of bad-weather data prevent us from drawing any strong conclusions.

One test of the self-consistency of our results is the condition (by definition) on the slopes that within experimental error,

$$F_\alpha \equiv \frac{\alpha_{10,33}\alpha_{33,90}}{\alpha_{10,90}} = 1. \tag{9}$$

For our Berkeley measurements, $F_\alpha = 0.95 \pm 0.10$. Our White Mountain results yield the value $F_\alpha = 0.99 \pm 0.12$. Both of these values indicate a good self-consistency.

5. DISCUSSION

The calculations displayed in Figures 1 and 2 result from a program based on the model by Waters [1976] modified to account for first-order interference effects [Rosenkranz, 1975] among the 60 GHz oxygen complex lines. The non-resonant term derived by Rosenkranz was also used. The calculations use the 1976 Standard Atmosphere [NOAA *et al.*, 1976] for the altitude dependencies of pressure and temperature. For the atmospheric emissions at an altitude of 250 m this model

Quantity	Experimental Value	Calculated Value These Results
$\alpha_{10,33}$	0.17±0.01	0.13
$\beta_{10,33}$	0.3±0.2	1.2
$\alpha_{10,90}$	0.047±0.004	0.022
$\beta_{10,90}$	0.9±0.2	1.8
$\alpha_{33,90}$	0.26±0.01	0.18
$\beta_{33,90}$	3.27±0.15	4.89

Table 1: Comparison of Results with Theoretical Expectations for an altitude of 250 m. Measurements were performed in Berkeley, California. The β's are in units of Kelvin.

yields:

$$\begin{aligned} 10.0\ GHz: &\quad T_{A,atm}(0) = 2.01 + 0.065\,W \\ 33.0\ GHz: &\quad T_{A,atm}(0) = 6.69 + 0.516\,W \\ 90.0\ GHz: &\quad T_{A,atm}(0) = 10.1 + 2.89\,W. \end{aligned} \tag{10}$$

Using relations (8a) and (8b), we may compare these values to the measured correlations. Table 1 summarizes the measured values and the model calculations for an altitude of 250 m.

For an altitude of 3800 m our model yields:

$$\begin{aligned} 10.0\ GHz: &\quad T_{A,atm}(0) = 0.894 + 0.044\,W \\ 33.0\ GHz: &\quad T_{A,atm}(0) = 2.98 + 0.366\,W \\ 90.0\ GHz: &\quad T_{A,atm}(0) = 4.55 + 2.18\,W. \end{aligned} \tag{11}$$

These are to be compared with previous calculations by Partridge *et al.* [1984] since a very similar model was employed. Partridge *et al.* [1984] obtained the following results for an altitude of 3800 m:

$$\begin{aligned} 10.0\ GHz: &\quad T_{A,atm}(0) = 1.048 + 0.040\,W \\ 33.0\ GHz: &\quad T_{A,atm}(0) = 3.182 + 0.360\,W \\ 90.0\ GHz: &\quad T_{A,atm}(0) = 4.706 + 2.197\,W, \end{aligned} \tag{12}$$

with uncertainties of 100 mK, 200 mK and 500 mK, respectively. Our calculations agree well with the calculations of Partridge *et al.* The major discrepancies lie in the oxygen terms since different non-resonant terms were used. More recent calculations (Liebe, personal communication, 1985), using for the most part relations and data presented in Liebe [1981], yield

$$\begin{aligned} 10.0\ GHz: &\quad T_{A,atm}(0) = 1.046 + 0.041\,W \\ 33.0\ GHz: &\quad T_{A,atm}(0) = 3.361 + 0.458\,W \\ 90.0\ GHz: &\quad T_{A,atm}(0) = 5.385 + 2.195\,W. \end{aligned} \tag{13}$$

Quantity	Experimental Value	Calculated Value		
		Partridge *et al.*	Liebe	These Results
$\alpha_{10,33}$	0.118±0.008	0.111	0.090	0.120
$\beta_{10,33}$	0.59±0.09	0.70	0.35	0.54
$\alpha_{10,90}$	0.028±0.003	0.018	0.019	0.020
$\beta_{10,90}$	0.82±0.14	0.96	0.95	0.80
$\alpha_{33,90}$	0.24±0.01	0.16	0.21	0.17
$\beta_{33,90}$	1.87±0.13	2.41	2.24	2.21

Table 2: Comparison of Results with Theoretical Expectations for an elevation of 3800 m. The β's are in units of Kelvin.

As one can see, these calculations agree fairly well with each other except for the water contributions at 33 GHz and 90 GHz and the oxygen contribution at 90 GHz. The uncertainties in the interference coefficients and the incomplete understanding of the excess water absorption limit the accuracy of these equations especially at the higher frequencies. By eliminating W from equations (11–13), we can compare these calculations with our experimental results. Table 2 summarizes the measured and calculated values for an altitude of 3800 m.

Our measurements in themselves do not allow one to ascertain directly the oxygen and water contributions at each frequency. We must have some foreknowledge of at least one a_ν and one b_ν. Tables 1 and 2 reveal that the agreement between the model calculations and our measurements is rather mixed. One notices that the agreement is better at the lower frequencies which are farther removed from the oxygen and water lines. The major discrepancies in Table 2 may explained if the calculated water attenuation at 90 GHz is too large. A value of $b_{90} = 1.54$ K/mm-water for our model (11) would result in substantial agreement for all of the slopes and intercepts. An overestimate of the water contribution at 90 GHz could be caused by the Gaut and Raufenstein empirical term, which differs from that of Liebe [1981; personal communication, 1985], especially in its frequency dependence.

The oxygen contribution at 10 GHz is dominated by the non-resonant term. The contributions as calculated by Partridge *et al.* and by Liebe (equations 12 and 13) are consistent with the lowest atmospheric emission measured at 10 GHz (1.02±0.12) whereas our calculations, using the non-resonant term of Rosenkranz, reveal a contribution somewhat lower but not necessarily inconsistent with our measurements. Previous low-frequency measurements ($<$ 10 GHz) also indicate that the Rosenkranz non-resonant oxygen term underestimates the oxygen attenuation at these frequencies (see Figure 2).

That Table 2 shows much better internal agreement than Table 1 could also partly be explained by the empirical term. One notices that all of the calculated slopes in Table 1 are much smaller than the measured values. This again perhaps reflects a tendency for calculations to overestimate the water contribution, but this time not just at 90 GHz.

Although an overestimate of the water contributions would account for many of the discrepancies observed in Table 1, substituting the measured slopes into equation (8b) reveals further discrepancies presumably due to the oxygen terms. The uncertainty in the temperature dependence of the linewidths of the oxygen lines could in part account for the discrepancy [Rosenkranz, 1975]. As Lam notes [1977], the validity of the impact approximation, especially for water vapor at higher pressures, is also somewhat questionable. The insolvability of many-body problems in quantum mechanics presently hinders calculations which do not use the impact approximation. That the impact approximation is more justifiable at lower pressures could account for both the agreement between the measured and calculated values in Table 2 and the disagreement of the values in Table 1. Interference effects (calculated by Rosenkranz to the first order) perhaps increase the discrepancies shown in Table 1. Another more tangible cause of the discrepancy between our measurements and calculations, especially at higher frequencies, could be the uncertainty in the interference constants for the oxygen lines (Danese, unpublished, 1984). Indeed Liebe [1981] notes that for at least two transitions the specific attenuation as calculated using Rosenkranz's first order theory become negative for frequencies larger than 160 GHz.

In general, our White Mountain results and our Berkeley results both reflect the need for an increased understanding of the microwave spectral behavior of the atmosphere. The discrepancy between the experimental and calculated values of the relative oxygen and water vapor dependencies could be the result of many factors. The most obvious shortcoming of existing theories is the inability to explain the excess absorption observed in the window regions. An overestimated water attenuation appears to be the major source of discrepancy between calculated and measured correlations, especially at higher frequencies. Although many measurements of atmospheric attenuation and emission under 100 GHz already exist [Crane, 1981], the simultaneous nature of our measurements will provide very good constraints on future models of atmospheric attenuation and emission, especially in the window regions where the discrepancy is the greatest.

Acknowledgements: The authors wish to thank the staff of the White Mountain Research Station, Hal Dougherty, Jon Aymon, Janice Gates, Mark Griffith, Bruce Grossan, Linda Kelley, Steve Levin and Faye Mitschang for their assistance. This work has been supported by National Science Foundation Grants No. PHY80-15694 and AST 800737 and the Department of Energy Contract DE-AC03-76SF00098.

REFERENCES

Crane, R., Fundamental limitations caused by RF propagations, *Proc. IEEE, 69*(2), 196-209, 1981.

De Amici, G., C. Witebsky, G. Smoot and S. Friedman, Measurements of the cosmic background radiation temperature at 3.3 and 9.1 mm, *Phys. Rev. D, 29*, 2673-2676, 1984.

Ewing, R. A., B. F. Burke, and D. H. Staelin, Cosmic background measurements at a wavelength of 9.24 mm, *Phys. Rev. Lett., 19*, 1251-1253, 1967.

Friedman, S. D., G.F. Smoot, G. De Amici, and C. Witebsky, A measurement of the cosmic background radiation temperature at 3.0 cm, *Phys. Rev. D, 29*, 2677-2679, 1984.

Lam, K. S., Application of pressure broadening theory to the calculation of atmospheric oxygen and water vapor microwave absorption, *J. Quant. Spectros. Radiat. Transfer. 17*, 351-383, 1977.

Liebe, H. J., Modelling attenuation and phase of radio waves in air at frequencies below 1000 GHz, *Radio Sci., 16*(6), 1183-1199, 1981.

Mandolesi, N., P. Calzolari, S. Cortiglioni, and G. Morigi, Measurement fo the cosmic background radiation temperature at 6.3 cm, *Phys. Rev. D, 29*(12), 2680–2682, 1984.

National Oceanic and Atmospheric Administration, National Aeronautics and Space Administration, and United States Air Force, *U.S. Standard Atmosphere, 1976*, NOAA–S/T 76–1562, U.S. Government Printing Office, 1976.

Partridge, R. B., J. Cannon, R. Foster, C. Johnson, E. Rubinstein, A. Rudolph, L. Danese and G. De Zotti, Automated measurement of the temperature of the atmosphere at 3.2 cm, *Phys. Rev. D, 29*(12), 2683–2685, 1984.

Rosenkranz, P. W., Shape of the 5 mm oxygen band in the atmosphere, *IEEE Trans. Antennas Propag., AP-23*(4), 498-506, 1975.

Sironi, G., P. Inzani, and A. Ferrari, Measurement of the cosmic background radiation at 6.3 cm, *Phys. Rev. D, 29*(12), 2680–2682, 1984.

Smoot, G. F., G. De Amici, S. Friedman, C. Witebsky, N. Mandolesi, Danese, and G. De Zotti, Low-Frequency measurements of the spectrum of the cosmic background radiation, *Phys. Rev. Lett., 51*, 1099-1104, 1983.

Smoot, G.F., G. De Amici, S. Levin and C. Witebsky, New measurements of the cosmic background radiation spectrum, Nuovo Cimento, ?, ?-?, 1985.

Stokes, R. A., R. B. Partridge, and D. T. Wilkinson, New measurements of the cosmic microwave background at $\lambda = 3.2$ cm and $\lambda = 1.58$ cm – evidence in support of a blackbody spectrum, *Phys. Rev. Lett., 19*, 1199-1202, 1967.

Ulaby, F. T., R. K. Moore, and A. K. Fung, *Microwave Remote Sensing: Active and Passive, Vol I: Microwave Remote Sensing Fundamentals and Radiometry*, pp. 256-343, Addison-Wesley, New York, 1981.

Waters, J. R., Absorption and emission by atmospheric gases, in *Methods of Experimental Physics*, vol. 12B, edited by M. L. Meeks, chapt. 2.3, Academic, New York, 1976.

Wilkinson, D.T., Measurement of the cosmic background at 8.65-mm wavelength, *Phys. Rev. Lett., 19*, 1195-1198, 1967.

LIST OF CAPTIONS

Figure 1: Calculated and measured vertical atmospheric emission as a function of frequency at an altitude of 250 m. Measurements were performed in Berkeley, California during clear weather.

Figure 2: Calculated and measured vertical atmospheric emission as a function of frequency at an altitude of 3800 m. Solid circles denote our measurements and open circles denote previous measurements [Wilkinson, 1967; Stokes *et al.*, 1967; Ewing *et al.* 1967; Mandolesi *et al.*, 1984; Sironi *et al.*, 1984]. All measurements were performed at the White Mountain Research Station during the summer. Solar hygrometer measurements performed in 1983 indicate that the precipitable water content is closer to 3 mm during clear summer weather.

Figure 3: Vertical atmospheric temperature at 10 and 33 GHz as measured from 250 m above sea level (Berkeley, CA). The best-fitting line drawn through the clear-weather data has a slope of 0.17 ± 0.01 and an intercept of 0.3 ± 0.2 K.

Figure 4: Vertical atmospheric temperature at 10 and 90 GHz as measured from 250 m above sea level (Berkeley, CA). The best-fitting line drawn through the clear-weather data has a slope of 0.042 ± 0.004 and an intercept of 0.9 ± 0.2 K.

Figure 5: Vertical atmospheric temperature at 33 and 90 GHz as measured from 250 m above sea level (Berkeley, CA). The best-fitting line drawn through the clear-weather data has a slope of 0.26 ± 0.01 and an intercept of 3.27 ± 0.15 K.

Figure 6: Vertical atmospheric temperature at 10 and 33 GHz as measured from 3800 m above sea level (White Mountain, CA). The best-fitting line drawn through the data has a slope of 0.12 ± 0.01 and an intercept of 0.59 ± 0.09 K.

Figure 7: Vertical atmospheric temperature at 10 and 90 GHz as measured from 3800 m above sea level (White Mountain, CA). The best-fitting line drawn through the data has a slope of 0.028 ± 0.003 and an intercept of 0.82 ± 0.14 K.

Figure 8: Vertical atmospheric temperature at 33 and 90 GHz as measured from 3800 m above sea level (White Mountain, CA). The best-fitting line drawn through the data has a slope of 0.24 ± 0.01 and an intercept of 1.87 ± 0.13 K.

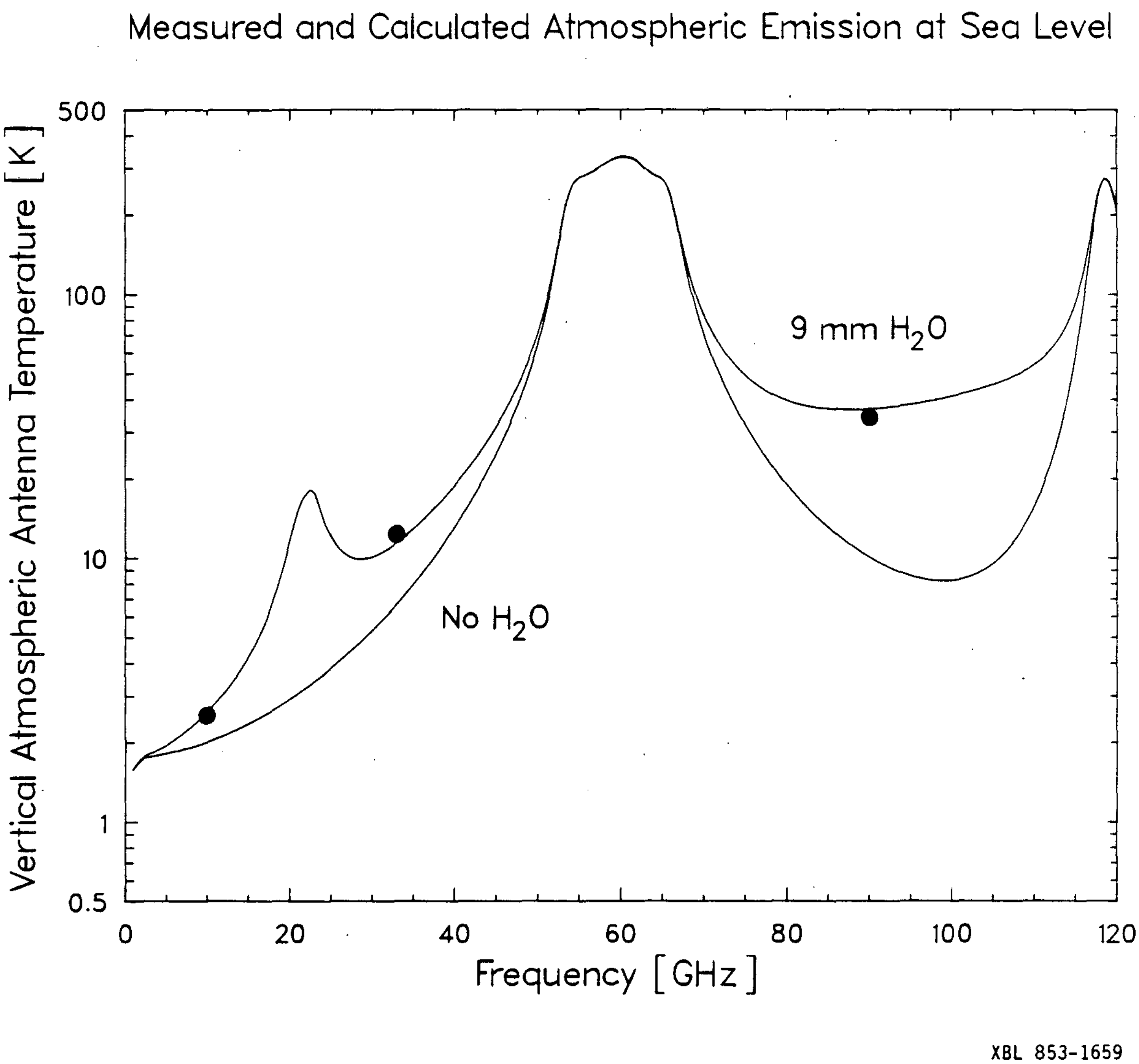

Figure 1: Calculated and measured vertical atmospheric emission as a function of frequency at an altitude of 250 m. Measurements were performed in Berkeley, California during clear weather.

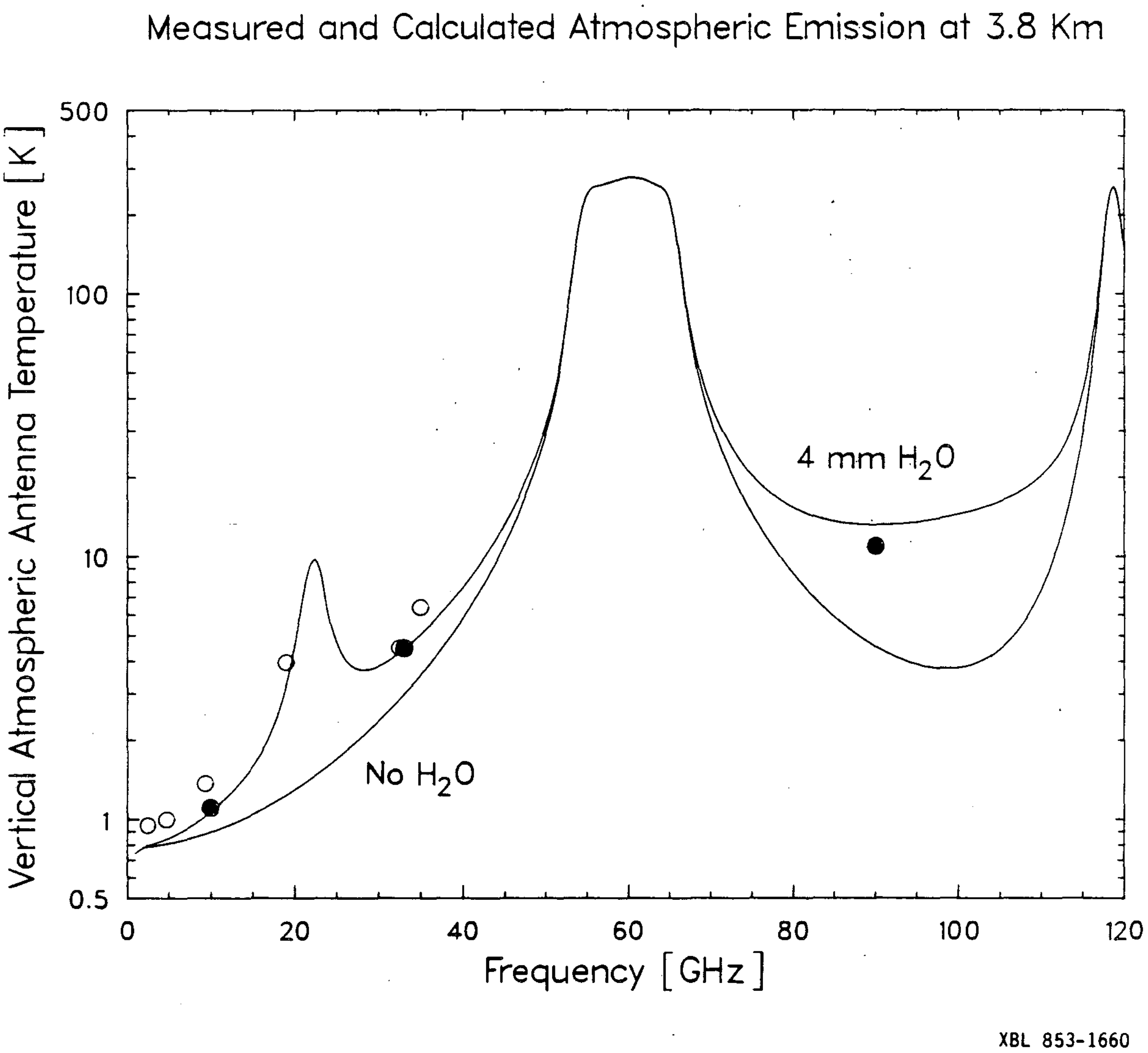

Figure 2: Calculated and measured vertical atmospheric emission as a function of frequency at an altitude of 3800 m. Solid circles denote our measurements and open circles denote previous measurements [Wilkinson, 1967; Stokes *et al.*, 1967; Ewing *et al.* 1967; Mandolesi *et al.*, 1984; Sironi *et al.*, 1984]. All measurements were performed at the White Mountain Research Station during the summer. Solar hygrometer measurements performed in 1983 indicate that the precipitable water content is closer to 3 mm during clear summer weather.

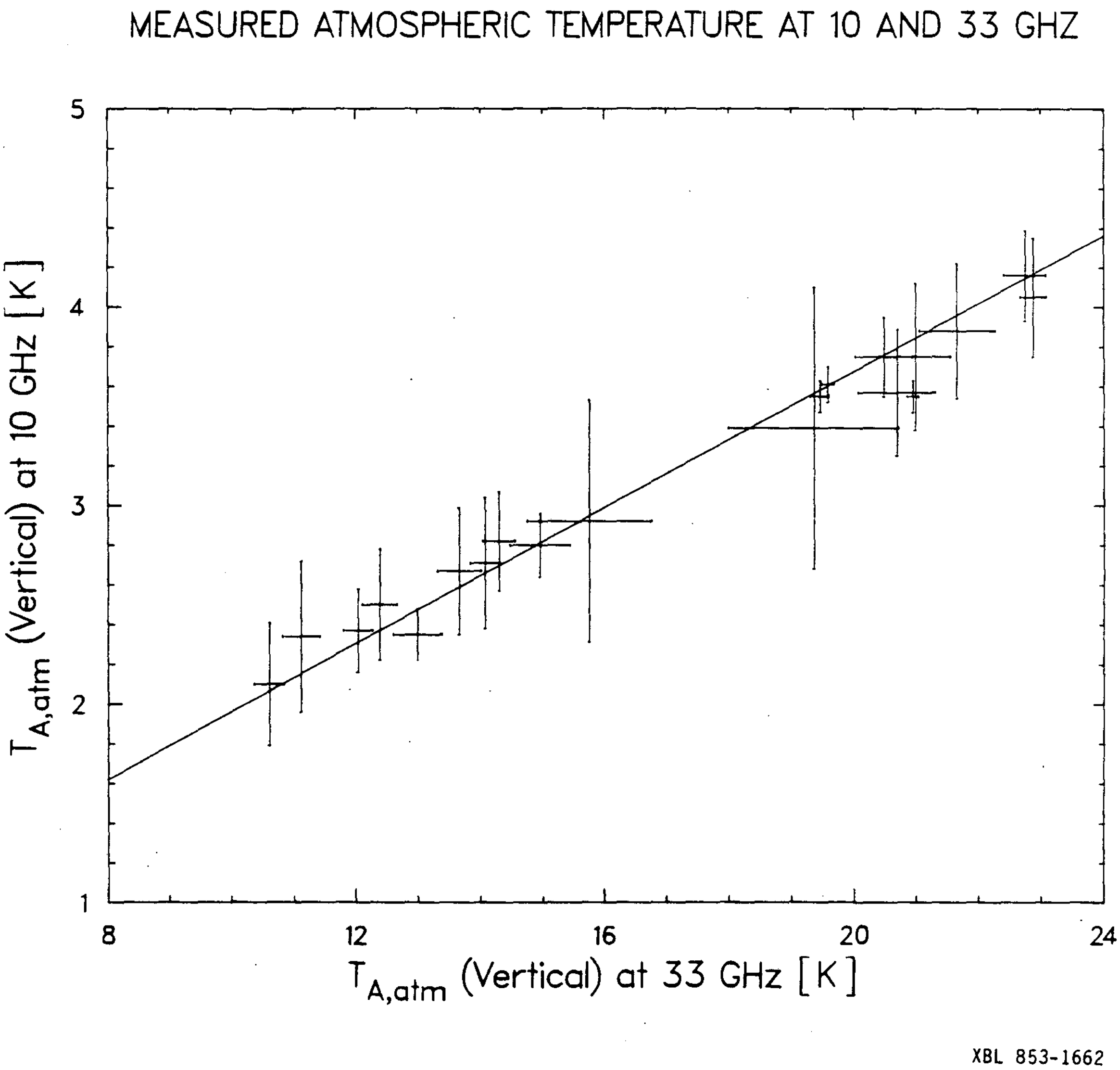

Figure 3: Vertical atmospheric temperature at 10 and 33 GHz as measured from 250 m above sea level (Berkeley, CA). The best-fitting line drawn through the clear-weather data has a slope of 0.17 ± 0.01 and an intercept of 0.3 ± 0.2 K.

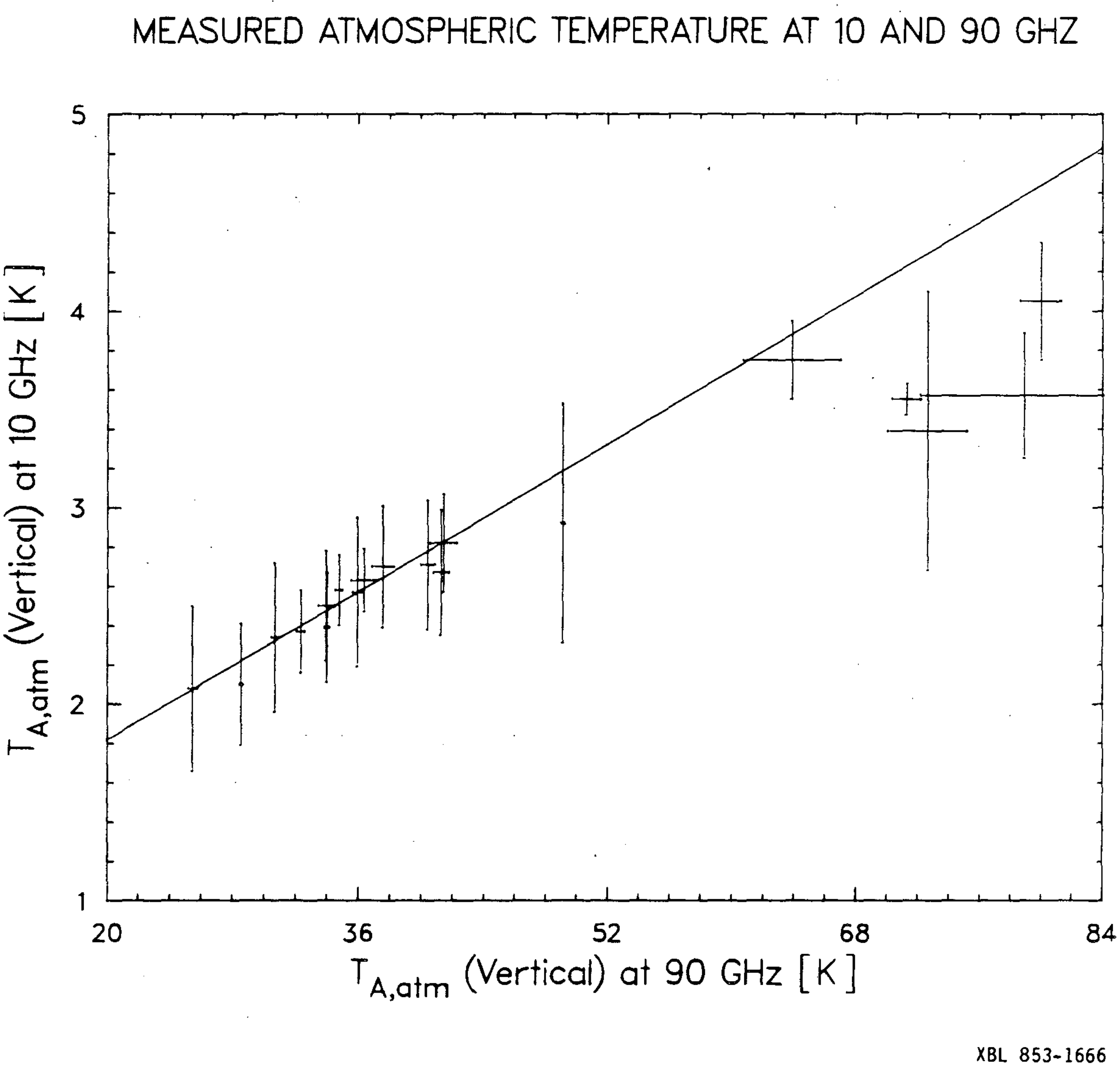

Figure 4: Vertical atmospheric temperature at 10 and 90 GHz as measured from 250 m above sea level (Berkeley, CA). The best-fitting line drawn through the clear-weather data has a slope of 0.042 ± 0.004 and an intercept of 0.9 ± 0.2 K.

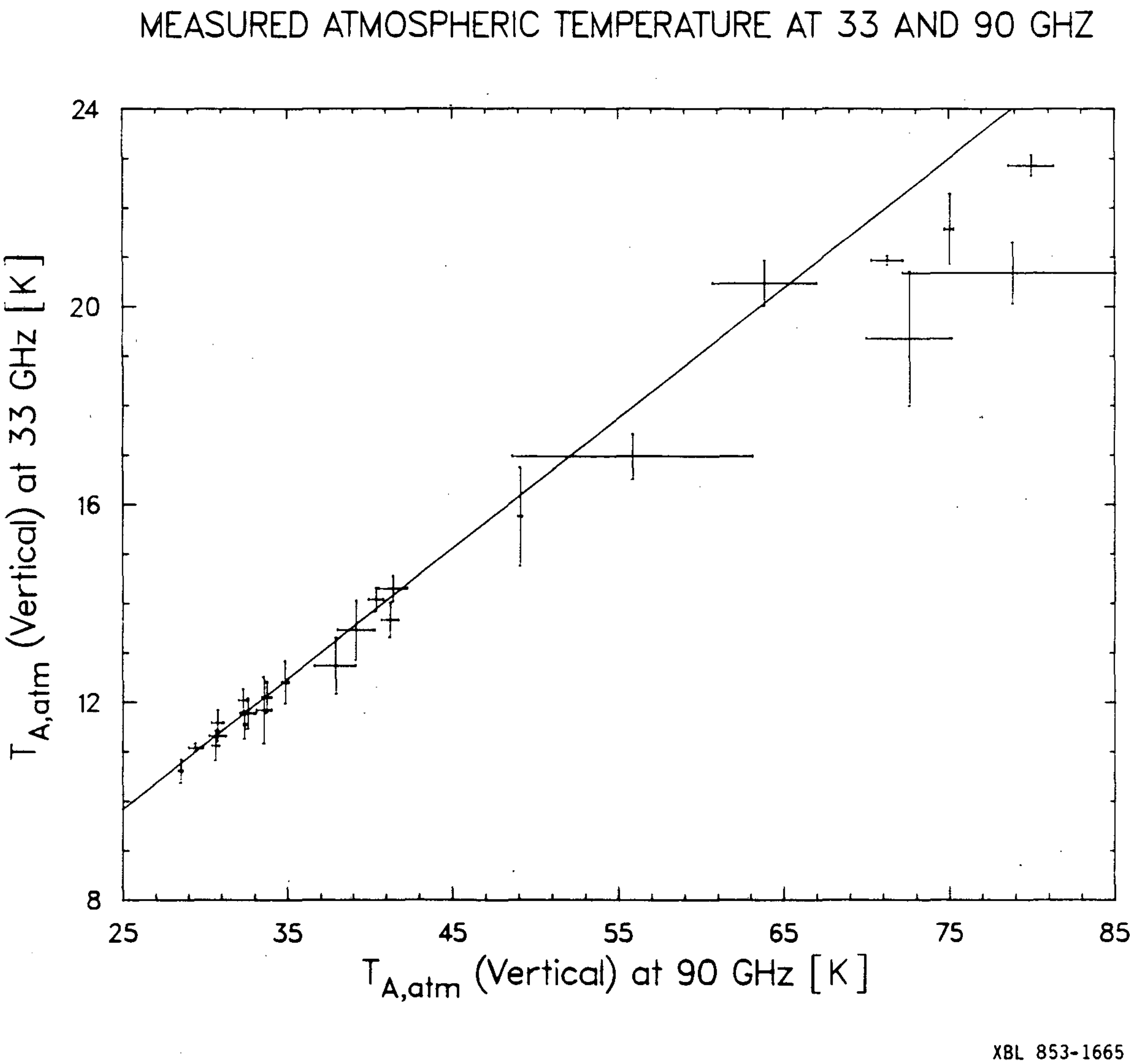

Figure 5: Vertical atmospheric temperature at 33 and 90 GHz as measured from 250 m above sea level (Berkeley, CA). The best-fitting line drawn through the clear-weather data has a slope of 0.26 ± 0.01 and an intercept of 3.27 ± 0.15 K.

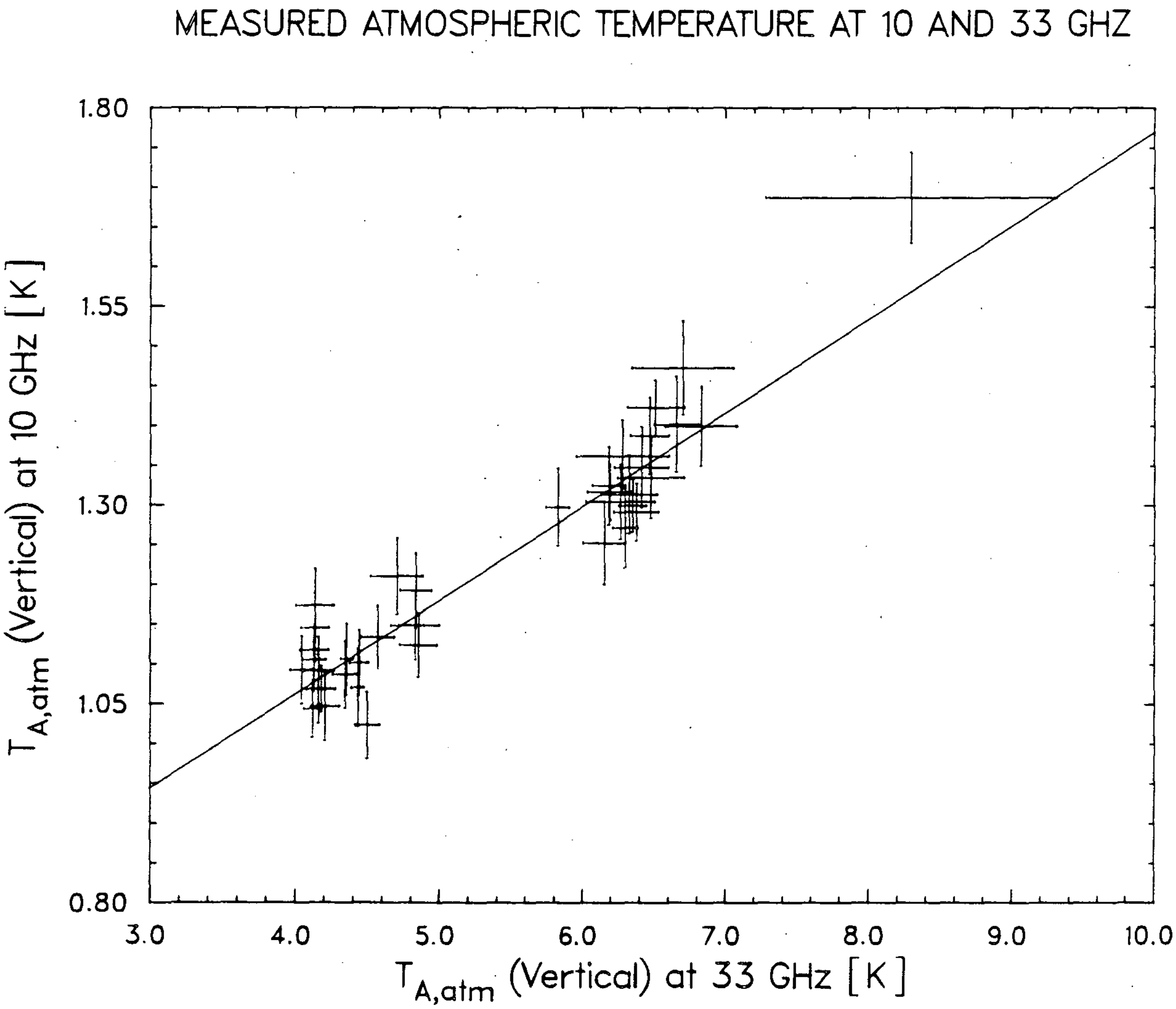

XBL 853-1664

Figure 6: Vertical atmospheric temperature at 10 and 33 GHz as measured from 3800 m above sea level (White Mountain, CA). The best-fitting line drawn through the data has a slope of 0.12 ± 0.01 and an intercept of 0.59 ± 0.09 K.

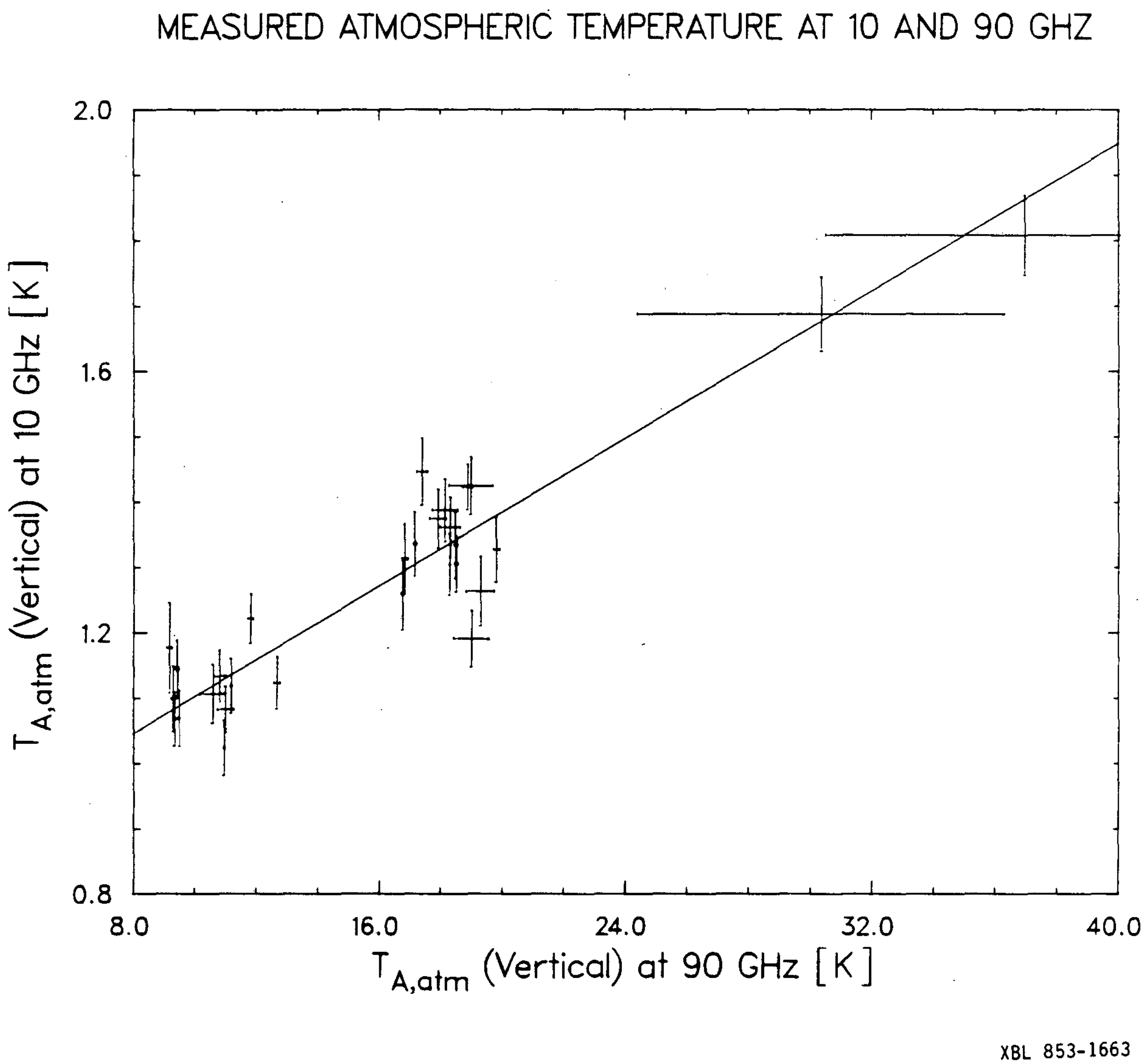

Figure 7: Vertical atmospheric temperature at 10 and 90 GHz as measured from 3800 m above sea level (White Mountain, CA). The best-fitting line drawn through the data has a slope of 0.028 ± 0.003 and an intercept of 0.82 ± 0.14 K.

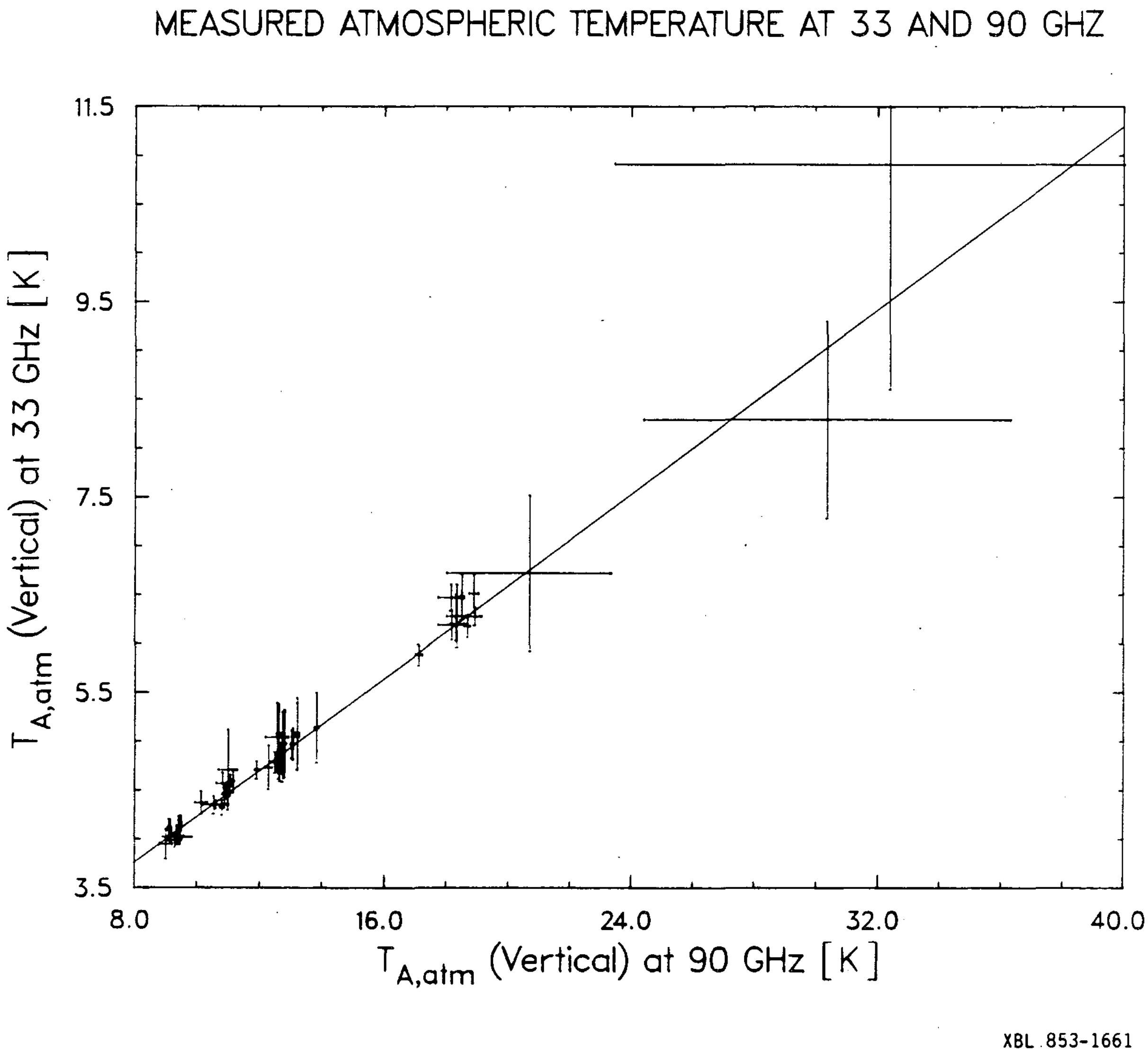

Figure 8: Vertical atmospheric temperature at 33 and 90 GHz as measured from 3800 m above sea level (White Mountain, CA). The best-fitting line drawn through the data has a slope of 0.24 ± 0.01 and an intercept of 1.87 ± 0.13 K.

LAWRENCE BERKELEY LABORATORY
TECHNICAL INFORMATION DEPARTMENT
UNIVERSITY OF CALIFORNIA
BERKELEY, CALIFORNIA 94720